Pressure exerted by a grafted polymer on the limiting line of a semi-infinite square lattice

2013 J. Phys. A: Math. Theor. 46 115004

(http://iopscience.iop.org/1751-8121/46/11/115004)

IOP PUBLISHING JOURNAL OF PHYSICS A: MATHEMATICAL AND THEORETICAL

J. Phys. A: Math. Theor. **46** (2013) 115004 (13pp) doi:10.1088/1751-8113/46/11/115004

Pressure exerted by a grafted polymer on the limiting line of a semi-infinite square lattice

Iwan Jensen[1], **Wellington G Dantas**[2], **Carlos M Marques**[3] **and Jürgen F Stilck**[4]

[1] ARC Centre of Excellence for Mathematics and Statistics of Complex Systems, Department of Mathematics and Statistics, the University of Melbourne, VIC 3010, Australia
[2] Departamento de Ciências Exatas, EEIMVR, Universidade Federal Fluminense, 27.255-125, Volta Redonda, RJ, Brazil
[3] Institut Charles Sadron, Université de Strasbourg, CNRS-UPR 22, 23 rue du Loess, F-67034 Strasbourg, France
[4] Instituto de Física and National Institute of Science and Technology for Complex Systems, Universidade Federal Fluminense, Av Litorânea s/n, Boa Viagem, 24.210-340, Niterói, RJ, Brazil

E-mail: jstilck@if.uff.br

Received 15 January 2013, in final form 30 January 2013
Published 27 February 2013
Online at stacks.iop.org/JPhysA/46/115004

Abstract
Using exact enumerations of self-avoiding walks (SAWs) we compute the inhomogeneous pressure exerted by a two-dimensional end-grafted polymer on the grafting line which limits a semi-infinite square lattice. The results for SAWs show that the asymptotic decay of the pressure as a function of the distance to the grafting point follows a power law with an exponent similar to that of Gaussian chains and is, in this sense, independent of excluded volume effects.

PACS numbers: 05.50.+q, 36.20.Ey

(Some figures may appear in colour only in the online journal)

1. Introduction

Imaging and manipulating matter at sub-micron length scales has been the cornerstone of nano-sciences development [1]. In soft matter systems, including those of biological relevance, the cohesive energies being only barely larger than the thermal energy k_BT, forces as small as a pico-Newton exerted over a nanometer length scale might be significant enough to induce structural changes. Examples can be found in the stretching of DNA molecules by optical traps [2], on the behavior of colloidal solutions under external fields [3] and on the deformations of self-assembled bilayers [4] to name just a few. Thus, in soft matter, when one exerts a localized force over a small area, precise control of the acting force requires not only a prescribed value

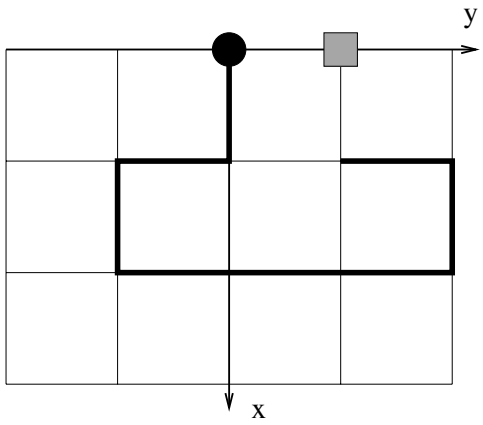

Figure 1. A self-avoiding walk (SAW) grafted at the origin $x = y = 0$ to a wall placed on the y axis. If the vertex on the wall at $(0, 1)$ is not excluded, the only possibility for the next step would be toward this vertex. If this vertex is excluded, the SAW will end at the final point $(1, 1)$.

of the total applied force but, more importantly, a precise pressure distribution in the contact area.

The microscopic nature of pressure has been understood since the seminal work of Bernoulli two and a half centuries ago: in a container, momentum is transferred by collisions from the moving particles to the walls [5]. When the particle concentration is homogeneous so is the pressure. Strategies for localizing the pressure over a nanometer area thus require the generation of strong concentration inhomogeneities, at equivalently small scales. Bickel *et al* [6, 7] and Breidnich *et al* [8] have recently realized that such inhomogeneities are intrinsic to entropic systems of connected particles such as polymer chains, and have computed the inhomogeneous pressure associated with end-grafted polymer chains within available analytical theories for ideal chains. Their results show that the polymer produces a local field of pressure on the grafting surface, with the interaction being strong at the anchoring point and vanishing far enough from it. Scaling arguments were also put forward in [7] to discuss the more relevant case of real polymer chains, where excluded volume interactions between the different monomers need to be taken into account. These arguments suggest that the functional variation of pressure with distance from the grafting point should be the same in chains with or without excluded volume interactions, albeit with different prefactors.

In this paper, we compute the inhomogeneous pressure applied to a wall by an end-grafted polymer with excluded volume interactions, modeled by self-avoiding walks (SAWs) on the square lattice. In figure 1, we illustrate our model with a wall located at $x = 0$. The wall is neutral, in the sense that the statistical weight of a monomer placed on the wall is equal to the weight of a monomer in the bulk. The length of a step of the walk is equal to the lattice constant a, and we use this as the length unit. The model is athermal, that is, all allowed configurations of a SAW have the same energy.

The canonical partition function of walks with n steps (Z_n) is equal to the number of SAWs starting at the origin and restricted to the half-plane $x \geqslant 0$, called $c_n^{(1)}$ in [9]. The Helmholtz free energy is given by $F_n = -k_B T \ln c_n^{(1)}$. We can estimate the pressure exerted by the SAW at a point $(0, r)$ on the wall by excluding this vertex from the lattice. The excluded vertex is represented as a hatched square in figure 1 at $r = 1$. The pressure $P_n(r)$ exerted at this point is then related to the change in the free energy when the vertex is excluded, $P_n a^2 = -\Delta F_n$. If we

call $c_n^{(1)}(r)$ the number of n step SAWs with the vertex at $(0, r)$ excluded, the dimensionless reduced pressure may be written as

$$p_n(r) = \frac{P_n(r)a^2}{k_B T} = -\ln \frac{c_n^{(1)}(r)}{c_n^{(1)}}. \tag{1}$$

Of course we are interested in the thermodynamic limit $p(r) = \lim_{n\to\infty} p_n(r)$, so the enumeration data must be extrapolated to the infinite length limit. It is worth noting that the density of monomers at the vertex $(0, r)$ is given by $\rho(r) = 1 - \lim_{n\to\infty} c_n^{(1)}(r)/c_n^{(1)}$, so that

$$p(r) = -\ln[1 - \rho(r)]. \tag{2}$$

The exact enumerations allow us to obtain precise estimates of the pressure exerted by SAWs at small distances of the grafting point, and we find, rather surprisingly, that the asymptotic form of this pressure is well reproduced even for these small values of r. In section 2, we give some details of the computational enumeration procedure. In section 3, the enumeration data are analyzed and estimates for the pressure as a function of the distance to the grafting point are presented. Final discussions and conclusions may be found in section 4.

2. Exact enumerations

The algorithm we use to enumerate SAWs on the square lattice builds on the pioneering work of Enting [10] who enumerated square lattice self-avoiding polygons using the finite lattice method. More specifically, our algorithm is based in large part on the one devised by Conway *et al* [11] for the enumeration of SAWs. The details of our algorithm can be found in [12]. Below we shall only briefly outline the basics of the algorithm and describe the changes made for the particular problem studied in this work.

The first terms in the series for the SAWs generating function can be calculated using transfer matrix (TM) techniques to count the number of SAWs in rectangles W vertices wide and L vertices long. Any SAW spanning such a rectangle has length at least $W + L - 2$. By adding the contributions from all rectangles of width $W \leqslant N+1$ and length $W \leqslant L \leqslant N-W+1$ the number of SAWs is obtained correctly up to length N.

The generating function for rectangles with fixed width W is calculated using TM techniques. The most efficient implementation of the TM algorithm generally involves bisecting the finite lattice with a boundary (this is just a line in the case of rectangles) and moving the boundary in such a way as to build up the lattice vertex by vertex as illustrated in figure 2. If we draw a SAW and then cut it by a line we observe that the partial SAW to the left of this line consists of a number of loops connecting two edges (we shall refer to these as loop ends) in the intersection, and pieces which are connected to only one edge (we call these free ends). The other end of the free piece is either the start-point or the end-point of the SAW so there are at most two free ends.

Each end of a loop is assigned one of two labels depending on whether it is the lower end or the upper end of a loop. Each configuration along the boundary line can thus be represented by a set of edge states $\{\sigma_i\}$, where

$$\sigma_i = \begin{cases} 0 & \text{empty edge,} \\ 1 & \text{lower loop-end,} \\ 2 & \text{upper loop-end,} \\ 3 & \text{free end.} \end{cases} \tag{3}$$

If we read from the bottom to the top, the configuration or signature S along the intersection of the partial SAW in figure 2 is $S = \{031\,212\,120\}$. Since crossings are not permitted this encoding uniquely describes which loop ends are connected.

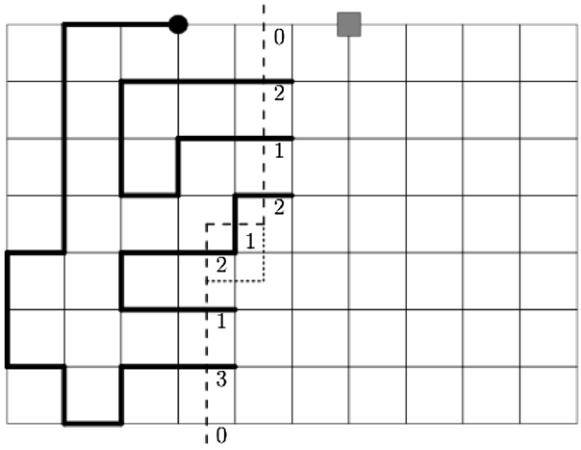

Figure 2. A snapshot of the boundary line (dashed line) during the transfer matrix (TM) calculation on a strip of width 7 with $r = 3$. The filled circle indicates the grafted start-point of the SAW and the shaded box the excluded vertex. SAWs are enumerated by successive moves of the kink in the boundary line, as exemplified by the position given by the dotted line, so that one vertex and two edges at a time are added to the strip. To the left of the boundary line we have drawn an example of a partially completed SAW.

The sum over all contributing graphs is calculated as the boundary is moved through the lattice. For each configuration of occupied or empty edges along the intersection we maintain a generating function G_S for partial walks with signature S. In exact enumeration studies such as this, G_S is a truncated polynomial $G_S(x)$, where x is conjugate to the number of steps. In a TM update, each source signature S (before the boundary is moved) gives rise to a few new target signatures S' (after the move of the boundary line) and $m = 0$, 1 or 2 new edges are inserted leading to the update $G_{S'}(x) = G_{S'}(x) + x^m G_S(x)$. Once a signature S has been processed it can be discarded. The calculations were performed using integer arithmetic modulo several prime numbers with the full integer coefficients reconstructed at the end using the Chinese remainder theorem.

Some changes to the algorithm described in [12] are required in order to enumerate the restricted SAW we study here. Grafting the SAW to the wall can be achieved by forcing the SAW to have a free end (the start-point) on the top side of the rectangle. In enumerations of unrestricted SAW, one can use symmetry to restrict the TM calculations to rectangles with $W \leqslant N/2 + 1$ and $L \geqslant W$ by counting contributions for rectangles with $L > W$ twice. The grafting of the start-point to the wall breaks the symmetry and we have to consider all rectangles with $W \leqslant N + 1$. Clearly the number of configurations one must consider grows with W. Hence, one wants to minimize the length of the boundary line. To achieve this, the TM calculation on the set of rectangles is broken into two subsets with $L \geqslant W$ and $L < W$, respectively. The calculations for the subset with $L \geqslant W$ are performed as outlined above. In the calculations for the subset with $L < W$, the boundary line is chosen to be horizontal (rather than vertical) so it cuts across at most $L+1$ edges. Alternatively, one may view the calculation for the second subset as a TM algorithm for SAW with its start-point on the left-most border of the rectangle.

Exclusion of the vertex at distance r from the starting point of the SAW is achieved by blocking this vertex so the walk cannot visit the vertex. The actual calculation can be performed in at least two ways. One can simply specify the position of the starting point (and r) on the upper/left border and sum over all possible positions. This means doing calculations for a given width W many times; once for each position of the starting point of the SAW. Alternatively,

one can introduce 'memory' into the TM algorithm. Specifically, once we have created a configuration which inserts the first free end we 'remember' that it did so. We can flag that the free end has been inserted by adding a ghost edge to the configuration initially in state 0. Once the first free end is inserted the state of the ghost edge is changed to 1. In the next sweep the state of the ghost edge is incremented by 1. When the state of the ghost edge has reached the value r the vertex on the top border is blocked. The problem with the first approach is that we need to do many calculations for any given rectangle. The problem with the second approach is that we need to keep $r+1$ copies of most TM configurations thus using substantially more memory. The choice will be a matter of whether the major computational bottle-neck is CPU time or memory. For this study, we used the first approach.

In more detail the TM algorithm for the case $L \geqslant W$ works as follows. A SAW has two free ends and in the TM algorithm the first free end is forced to be at the top at a distance k from the left border (this is the starting point of the SAW). We then add a further $r-1$ columns; in the next column the top vertex is forced to be empty. After this further columns are added up to a maximum length of $L_m = N - W + 1$. This calculation is then repeated for $k = 0$ to L_m thus enumerating all possible SAWs spanning rectangles of width exactly W and length $L \geqslant W$. A similar calculation is then performed with the SAW grafted to the left border and in each case repeated for all $W \leqslant N/2$.

The calculation above enumerates almost all possible SAWs. However, we have missed those SAWs with two free ends in the top border where the end-point precedes the starting-point. That is there is a free end in the top border at a distance $> r$ prior to the excluded vertex. We need to count such SAWs separately. The required changes to the algorithm are quite straightforward and will not be detailed here.

We calculated the number of SAWs up to length $n = 59$ for the unrestricted case and for an excluded vertex with $r = 1,\ 2,\ 3,\ 4,\ 5,\ 10, 20$. In each case, the calculation was performed in parallel using up to eight processors, a maximum of some 16 GB of memory and using a total of under 2000 CPU hours (see [12] for details of the parallel algorithm). We needed three primes to represent each series correctly and the calculations for all the primes were performed in a single run.

3. Analysis and results

In tables 1 and 2, we have listed the results for the enumerations of SAWs without additional restrictions, $c_n^{(1)}$, and walks which are not allowed to occupy the vertex $(0, 1)$ of the wall, $c_n^{(1)}(1)$. If we calculate the pressures directly, we note a parity effect, as seen in the results presented in figure 3. This effect is related to an unphysical singularity in the generating function of the counts $c_n^{(1)}$, $G(x) = \sum_{n=0}^{\infty} c_n^{(1)} x^n$. Besides the physical singularity at $x = x_c = 1/\mu$, where μ is the connective constant, there is another singularity at $x = -1/\mu$ [9]. This point will be discussed in more detail below, and more precise estimates for the pressures at several distances from the grafting point will be provided.

3.1. Critical points and exponents

The critical behavior of a polymer grafted to a surface is well established [13]. It has been proved that the connective constant of grafted walks equals that of unrestricted walks [14]. The associated generating function has a dominant singularity at $x = x_c = 1/\mu$

$$G(x) = \sum_n c_n^{(1)} x^n \sim A(1 - \mu x)^{-\gamma_1}, \tag{4}$$

where $\gamma_1 = 61/64$ is a known [15, 16] critical exponent. Besides the physical singularity there is another singularity at $x = x_- = -x_c$ [17, 9].

Table 1. Number of walks in the half-plane $c_n^{(1)}$.

n	$c_n^{(1)}$	n	$c_n^{(1)}$	n	$c_n^{(1)}$
1	3	21	681 552 747	41	176 707 555 110 156 095
2	7	22	1793 492 411	42	465 629 874 801 142 259
3	19	23	4725 856 129	43	1227 318 029 107 006 037
4	49	24	12 439 233 695	44	3234 212 894 649 555 857
5	131	25	32 778 031 159	45	8525 055 738 741 918 835
6	339	26	86 295 460 555	46	22 466 322 857 670 716 727
7	899	27	227 399 388 019	47	59 220 537 922 987 286 933
8	2345	28	598 784 536 563	48	156 073 168 859 898 607 113
9	6199	29	1577 923 781 445	49	411 414 632 591 966 686 887
10	16 225	30	4155 578 176 581	50	1084 313 600 069 268 939 547
11	42 811	31	10 951 205 039 221	51	2858 360 190 045 390 998 925
12	112 285	32	28 844 438 356 929	52	7533 725 151 809 823 220 637
13	296 051	33	76 016 486 583 763	53	19 860 118 923 927 104 821 817
14	777 411	34	200 242 023 748 929	54	52 346 889 766 180 530 489 735
15	2049 025	35	527 735 162 655 901	55	137 997 896 899 080 793 506 959
16	5384 855	36	1390 287 671 021 273	56	363 744 527 134 008 049 572 583
17	14 190 509	37	3664 208 598 233 159	57	958 930 393 586 321 187 515 995
18	37 313 977	38	9653 950 752 700 371	58	2527 696 511 232 818 406 275 131
19	98 324 565	39	25 444 550 692 827 111	59	6663 833 305 674 862 002 802 763
20	258 654 441	40	67 042 749 110 884 297		

Table 2. Number of restricted walks in the half-plane $c_n^{(1)}(1)$.

n	$c_n^{(1)}(1)$	n	$c_n^{(1)}(1)$	n	$c_n^{(1)}(1)$
1	2	21	484 553 893	41	125 845 983 216 200 025
2	5	22	1277 403 184	42	331 741 159 147 128 245
3	13	23	3361 118347	43	874 112 388 226 242 422
4	35	24	8860 136 085	44	2304 278 197 456 842 952
5	91	25	23 319 106 552	45	6071 977 423 574 762 560
6	242	26	61 468 398 004	46	16 006 835 327 039 914 244
7	630	27	161 814 936 995	47	42 181 825 940 070 651 834
8	1672	28	426 530 787 110	48	111 200 914 189 945 767 681
9	4369	29	1123 043 680 259	49	293 056 004 233 059 019 257
10	11 558	30	2960 232 320 818	50	772 575 890 795 109 134 325
11	30 275	31	7795 418 415 398	51	2036 121 996 024 316 003 415
12	79 967	32	20 548 006 324 647	52	5367 866 589 569 286 706 072
13	209 779	33	54 117 914 172 220	53	14 147 607 361 624 429 924 807
14	553 634	34	142 651 034 798 697	54	37 298 221 266 819 312 654 286
15	1453 801	35	375 747 632 401 071	55	98 307 470 253 293 931 954 939
16	3834 878	36	990 456 507 011 029	56	259 178 303 320 281 122 974 230
17	10 077 384	37	2609 158 017 850 105	57	683 144 867 659 867 533 730 505
18	26 574 366	38	6877 742 334 133 961	58	1801 074 652 042 354 959 971 779
19	69 870 615	39	18 119 629 209 950 641	59	4747 450 605 648 675 761 162 683
20	184 216 886	40	47 764 129 557 587 369		

We have analyzed the series using differential approximants [18]. We calculate many individual approximants and obtain estimates for the critical points and exponents by an averaging procedure described in [19, chapter 8]. Here and elsewhere uncertainties on estimates from differential approximants were obtained from the spread among the various approximants as detailed in [19]. The results for unrestricted grafted SAWs are listed in table 3 under $r = 0$. We also list estimates for the cases $r = 1,\ 2,\ 5$ and 10. From these estimates, it is clear that

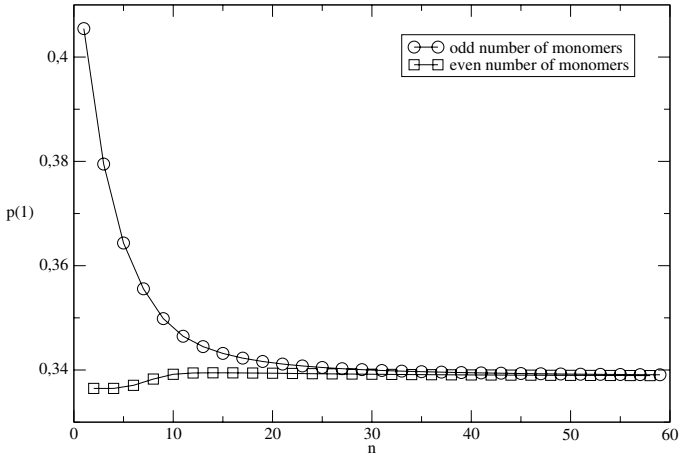

Figure 3. Pressure $p_n(r)$ for $r = 1$, calculated with the enumeration data for $c_n^{(1)}$ and $c_n^{(1)}(1)$ using expression (1).

Table 3. Estimates of the critical points and exponents for SAWs with an excluded vertex a distance r from the origin ($r = 0$ is the unrestricted case). The estimates were obtained from third-order approximants with L being the degree of the inhomogeneous polynomial.

r	L	x_c	γ	x_-	γ_-
0	0	0.379 052 260(64)	0.953 097(70)	−0.379 0526(38)	1.5002(19)
0	4	0.379 052 241(20)	0.953 072(17)	−0.379 0492(30)	1.5023(13)
0	8	0.379 052 243(14)	0.953 071(15)	−0.379 0498(21)	1.5016(12)
1	0	0.379 052 2582(30)	0.953 0884(24)	−0.379 0425(97)	1.5074(74)
1	4	0.379 052 2575(38)	0.953 0879(30)	−0.379 030(26)	1.523(29)
1	8	0.379 052 257(11)	0.953 090(14)	−0.379 058(16)	1.4988(69)
2	0	0.379 052 292(16)	0.953 123(13)	−0.379 0511(33)	1.5011(24)
2	4	0.379 052 276(12)	0.953 1115(97)	−0.379 0478(89)	1.5036(60)
2	8	0.379 052 306(26)	0.953 135(20)	−0.379 057(21)	1.498(20)
5	0	0.379 052 18(21)	0.953 04(17)	−0.379 114(61)	1.457(37)
5	4	0.379 052 25(31)	0.953 13(24)	−0.379 099(40)	1.467(29)
5	8	0.379 052 26(29)	0.953 13(25)	−0.379 074(31)	1.482(20)
10	0	0.379 0483(12)	0.9494(12)	−0.379 230(55)	1.369(32)
10	4	0.379 0493(40)	0.9503(32)	−0.379 237(29)	1.369(14)
10	8	0.379 0508(22)	0.9514(14)	−0.379 246(91)	1.365(54)

all the series have the same critical behavior. That is a dominant singularity at $x = x_c$ with exponent $-\gamma_1 = -61/64$ and a non-physical singularity at $x = x_- = -x_c$ with a critical exponent consistent with the exact value $\gamma_- = 3/2$.

The critical behavior can be established more rigorously from a simple combinatorial argument. The number of walks $c_n^{(1)}(r)$ with the point at $(0, r)$ excluded is clearly less than the number of unrestricted walks $c_n^{(1)}$. On the other hand, if we attach a single vertical step to the grafting point of an unrestricted walk, we obtain a walk which does not touch the surface at all and hence these walks are a subset of $c_n^{(1)}(r)$. This establishes the inequality

$$c_{n-1}^{(1)} \leqslant c_n^{(1)}(r) \leqslant c_n^{(1)}, \tag{5}$$

and hence shows that up to amplitudes the asymptotic behaviors of these sequences are identical.

3.2. Pressure

Having established the critical behavior of the series we can now turn to the determination of the pressure exerted by the polymer on the surface. Since all the series have the same dominant critical behavior it follows from (1) that the pressure is given by the ratio of the critical amplitudes.

One way of estimating the amplitudes is by a direct fit to an assumed asymptotic form. Here we assume that the asymptotic behavior of our series is similar to that of unrestricted SAW [20]. The asymptotic analysis of [20] was very thorough and clearly established that the leading non-analytic correction-to-scaling exponent has the value 3/2 (there are also analytic, i.e. integer valued corrections to scaling). We repeated some of the steps in this analysis with the same result for the leading non-analytic correction-to-scaling exponent. Naturally, there may be further non-analytic correction-to-scaling exponents with values $> 3/2$, but these would be impossible to detect numerically with any degree of certainty. So here we assume that the physical singularity has a leading correction-to-scaling exponent of 1 followed by further half-integer corrections, while we assume only integer corrections at the non-physical singularity. We thus fit the coefficients to the asymptotic form

$$c_n^{(1)}(r) = \mu^n \left[n^{\gamma_1 - 1} \left(A(r) + \sum_{j=2} a_j(r)/n^{j/2} \right) + (-1)^n n^{-\gamma_- - 1} \sum_{k=0} b_k(r)/n^k \right]. \tag{6}$$

In the fits we use the extremely accurate estimate $\mu = 2.638\,158\,530\,35(2)$ obtained from an analysis of the series for self-avoiding polygons on the square lattice [21] and the conjectured exact values $\gamma_1 = 61/64$ and $\gamma_- = 3/2$. That is, we take a sub-sequence of terms $\{c_n^{(1)}(r), c_{n-1}^{(1)}(r), \ldots, c_{n-2m-1}^{(1)}(r)\}$, plug into the formula above taking m terms from both the a_j and b_k sums, and solve the $2m$ linear equations to obtain estimates for the amplitudes.

It is then advantageous to plot estimates for the leading amplitude $A(r)$ against $1/n$ for several values of m as done in figure 4. The behavior of the estimates for the leading amplitudes shown in this figure supports that (6) is a very good approximation to the true asymptotic form. In particular, note that the slope becomes very flat as n is increased and decreases as the number of terms m included in the fit is increased. From these plots, we estimate $A = 1.124\,705(5)$, $A(1) = 0.801\,625(5)$, $A(2) = 0.975\,64(2)$ and $A(5) = 1.093\,25(10)$, where the uncertainty is a conservative value chosen to include most of the extrapolations from figure 4.

The amplitude ratios $A(r)/A$, and hence the pressure, can also be estimated by direct extrapolation of the relevant quotient sequence, using a method due to Owczarek *et al* [22]: given a sequence $\{a_n\}$ defined for $n \geqslant 1$, assumed to converge to a limit a_∞ with corrections of the form $a_n \sim a_\infty(1 + b/n + \cdots)$, we first construct a new sequence $\{p_n\}$ defined by $p_n = \prod_{m=1}^{n} a_m$. We then analyze the corresponding generating function

$$P(x) = \sum p_n x^n \sim (1 - a_\infty x)^{-(1+b)}.$$

Estimates for a_∞ and the parameter b can then be obtained from differential approximants, that is a_∞ is just the reciprocal of the first singularity on the positive real axis of $P(x)$. In our case, we study the sequence of ratios $a_n(r) = c_n^{(1)}(r)/c_n^{(1)}$, which has the required asymptotic form. Using the same type of differential approximant method outlined above, we find that $A/A(1) = 1.403\,0218(5)$, which is entirely consistent with the estimate $A/A(1) = 1.403\,030(15)$ obtained using the amplitude estimates from the direct fitting procedure.

Next we compare these results for the pressure with the ones for Gaussian chains as expressed in equation (4) in [6]. That expression is for polymers in a three-dimensional half-space confined by a two-dimensional wall, and corresponds to finite values of the radius of

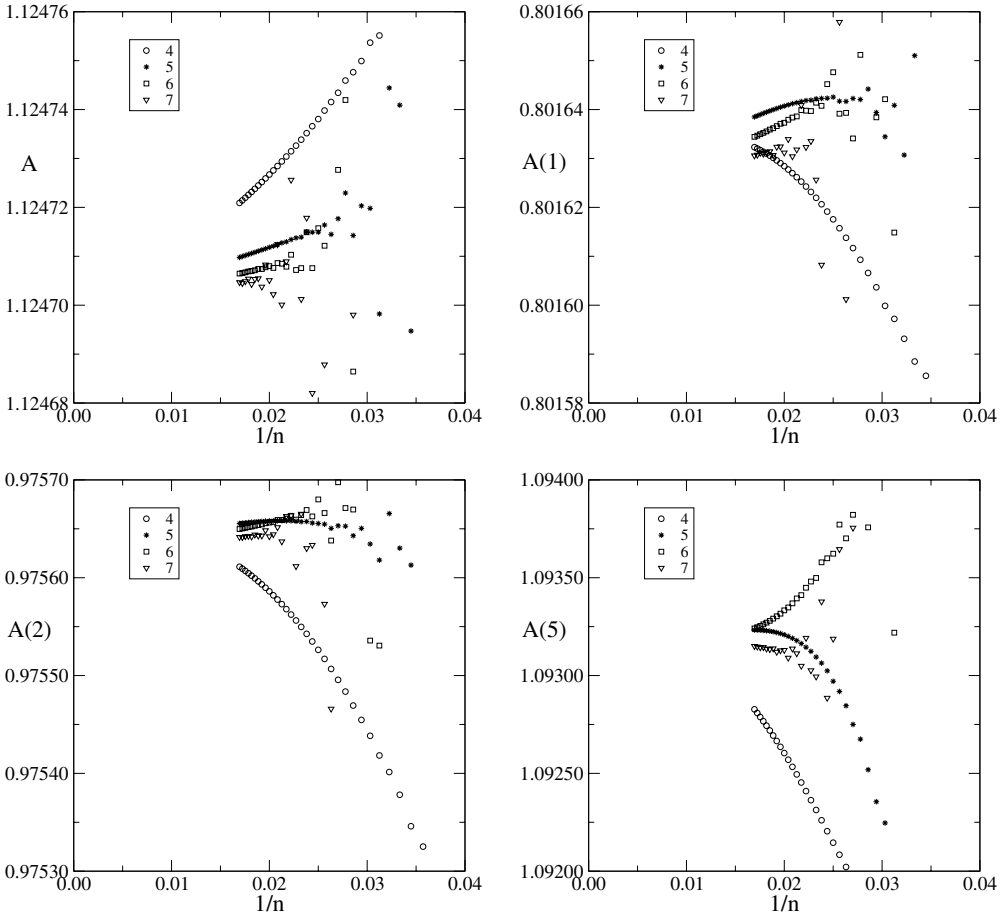

Figure 4. Estimates for the leading amplitudes obtained by fitting to the asymptotic form (6) plotted against $1/n$ while truncating the asymptotic expansion after 4 to 7 terms.

Table 4. Pressure at a distance r from the grafting point for SAWs and Gaussian chains.

r	$p(r)$-SAWs	$p(r)$-Gaussian
1	0.338 63	0.159 15
2	0.142 18	0.063 66
3	0.073 34	0.031 83
4	0.043 47	0.018 72
5	0.028 44	0.012 24
10	0.007 35	0.003 15

gyration. If the expression is generalized to the d-dimensional case and restricted to the limit of infinite chains, where the radius of gyration diverges, the result is

$$p_G(r) = \frac{P_G(r)a^d}{k_BT} = \frac{\Gamma(d/2)}{\pi^{d/2}} \frac{1}{(r^2+1)^{d/2}}, \tag{7}$$

where we recall that r is dimensionless, measured in units of the lattice constant a. In table 4, we have listed the estimated pressures for SAWs and the pressures obtained for Gaussian

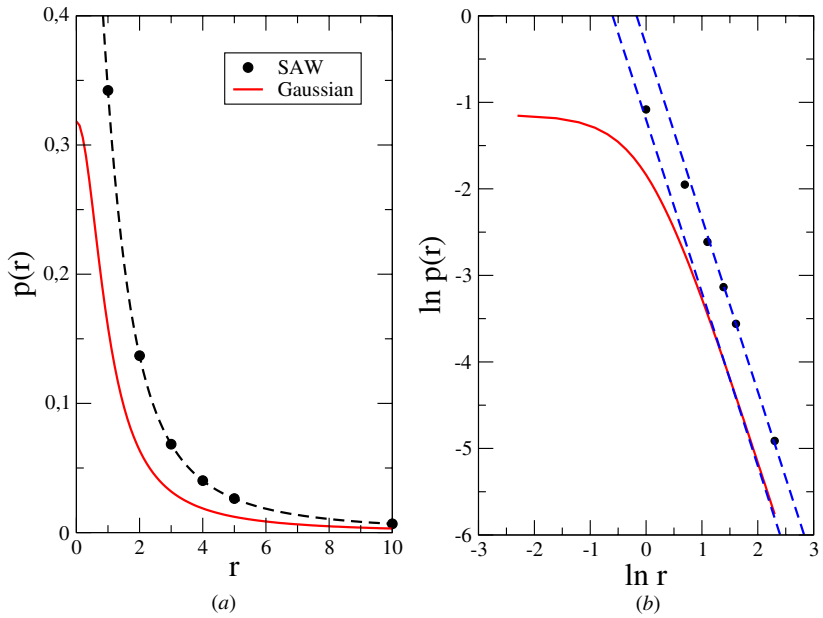

Figure 5. (*a*) The pressure $p(r)$ exerted by a polymer on a surface at a distance r from the grafting point. Data for polymers are modeled as SAWs or Gaussian chains. The dashed line is a $1/r^2$ fit. (*b*) Both data have the same $1/r^2$ scaling form, even for values close to $r = 2$. The dashed lines are guidelines with slope equal to -2.

chains in $d = 2$, on the semi-infinite square lattice. In figure 5, we have plotted the pressure for polymers modeled as SAWs and as Gaussian chains. In this figure, the dashed line represents a decay in pressure with the same asymptotic form, $\propto 1/(r^2 + 1)$, as the Gaussian chain but normalized so the curve passes through the SAWs data point for $r = 10$. Quite clearly the SAWs data are well represented by this form even for small distances $r > 2$. For $r = 20$, the SAWs data were indistinguishable from zero pressure.

4. Final discussions and conclusion

Since our model is athermal and discrete, it is not really possible to compare our results with those obtained for the Gaussian chain. However, as was already mentioned by Bickel *et al* [7], the excluded volume interactions should not change the scaling form of the pressure. Figure 5(*b*) clearly shows a $1/r^2$ decay of the pressure, even for small distances. According to Bickel *et al* [7], this similarity is due to the fact that the pressure and the monomer concentration in the vicinity of the wall are linearly related. On the other hand, it seems that the concentration is not affected by the molecular details or by the differences between chain models. In our case, despite the fact that $\rho(r)$ and $p(r)$ are related by a logarithmic relation, as shown in expression (2), we have for $r \gg 1$ a small concentration leading to a linear relation between those quantities. Actually, even for $r \sim 2$, we can observe a linear dependence, as shown in figure 6.

Since the grafted chain is in mechanical equilibrium, the force $\mathcal{F}$ applied to the walk at the grafting point, which is in the negative x direction in figure 1, should be equal to the sum

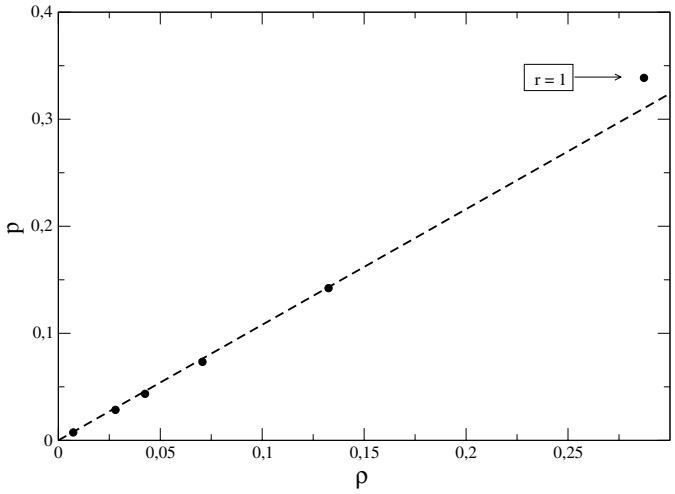

Figure 6. Relation between pressure and concentration of monomers near to the wall at a distance r from the grafting point. For $r > 1$, a linear relationship is observed.

of the forces applied by the wall at other contact points, which are in the positive x direction. Thus, the dimensionless force is given by

$$f = \frac{\mathcal{F}a}{k_B T} = 2\sum_{r=1}^{\infty} p(r). \tag{8}$$

For Gaussian chains, integrating equation (7), we find $f_G = 1$. For SAWs, we may estimate the force summing the results for $r = 1, 2, \ldots, 5$ and obtaining the remaining contributions ($r = 6, 7, \ldots, \infty$) using the asymptotic result $p(r) \approx A_p/(r^2 + 1)$, where $A_p \approx 0.742\,35$ was estimated using the result of $p(r)$ for $r = 10$. The result of this calculation is $f_{\mathrm{SAW}} \approx 1.533$, larger than the one for Gaussian chains. As mentioned above, it does not seem straightforward to compare the two models, since a Gaussian chain is a mass-spring model and therefore it is, unlike SAWs, not athermal. We may also mention that if $p(r)$ for SAWs is extended to real values of r using a numerical interpolation procedure and the data for Gaussian chains are rescaled so the areas below both curves are the same, the difference between the curves is quite small, the maximum being close to the origin and of order 10^{-3}. Due to the limited precision of the estimates for SAWs and to the expected small dependency of the results on the interpolation procedure, we will not present these results here, but we found that in general the rescaled results for the pressure of Gaussian chains are larger than the pressures for SAWs at small values of r, but the inverse situation is found for larger distances. This net effect may be understood if we recall that the pressure is a monotonically growing function of the local density at the wall (equation (2)) and that the effect of the excluded volume interactions should be a slower decay of this density with the distance from the grafting point, as compared to approximations where this interaction is neglected.

It is of some interest to obtain the total force applied to the chain at the grafting point for ideal chains, modeled by random walks on the semi-infinite square lattice. This force may be calculated considering the shift of the grafting point by one lattice unit in the positive x direction in figure 1. The change in free energy under this operation will be proportional to the force. These calculations should lead to the same result of the ones above, where the force was obtained summing over the pressures at all other sites of the wall besides the origin, since the total force applied on the chain has to vanish.

Let us start by briefly reviewing the calculation of the number of random walks on a half-plane of the square lattice. If we call $c_n(\vec{\rho})$ the number of n-step random walks on a square lattice starting at the origin and ending at the point $\vec{\rho} = x\mathbf{i} + y\mathbf{j}$, the number of RWs on the half-plane $x \geqslant 0$ may be calculated by placing an absorbing wall at $x = -1$, so that any walk reaching the wall is annihilated. This may be accomplished by using an image walker, starting at the reflection point of the origin with respect to the wall and ending at $\vec{\rho}$. We will place the starting point of the random walk at $(s, 0)$, where $s = 0$ corresponds to walks starting at the origin. In this case, the image walker starting point will be at $\vec{\rho}_0 = -(s+2)\mathbf{i}$, with distances measured in units of the lattice constant a. The number of walks confined to the $x \geqslant 0$ half plane is given by [23]

$$c_n^{(1)}(\vec{\rho}, s) = c_n(\vec{\rho}) - c_n(\vec{\rho} + (2+s)\mathbf{i}). \tag{9}$$

Since we are interested in the large n limit, we may use the Gaussian approximation for the number of walks

$$c_n(\vec{\rho}) = \frac{4^n}{n\pi} \exp\left(-\frac{|\vec{\rho}|^2}{n}\right). \tag{10}$$

For the half-plane, we obtain

$$c_n^{(1)}(\vec{\rho}, s) = \frac{4^n}{n\pi}\left[\exp\left(-\frac{|\vec{\rho}|^2}{n}\right) - \exp\left(-\frac{|\vec{\rho} + (2+s)\mathbf{i}|^2}{n}\right)\right]. \tag{11}$$

To obtain the total number of walks, we integrate this expression over the final point $\vec{\rho}$

$$c_n^{(1)}(s) = \int_0^\infty \mathrm{d}x \int_{-\infty}^\infty \mathrm{d}y\, c_n^{(1)}(\vec{\rho}, s). \tag{12}$$

The result is

$$c_n^{(1)}(s) = \frac{4^n}{\sqrt{\pi}} \int_{-s/\sqrt{n}}^{(2+s)/\sqrt{n}} \mathrm{e}^{-x^2} \mathrm{d}x, \tag{13}$$

for $n \gg s$, we have the asymptotic behavior

$$c_n^{(1)}(s) = 4^n \frac{2(s+1)}{\sqrt{n\pi}}, \tag{14}$$

which has the expected scaling form (4), with exponent $\gamma = 1/2$ and amplitude $A = 2(s+1)/\sqrt{\pi}$. The change in free energy between the cases with $s = 0$ and $s = 1$ is therefore given by $-k_B T \ln 2$, so that the force applied to the polymer by the wall at the grafting point will be $f_{\mathrm{RW}} = \ln 2 \approx 0.6931$, which is lower than the forces obtained for Gaussian chains and estimated for SAWs.

It should be mentioned that for SAWs the sum of the pressures corresponding to two distances $p(r_i) + p(r_j)$ is always smaller (for finite $|r_i - r_j|$) than $-\Delta F(r_i, r_j)/(k_B T)$, where $\Delta F(r_i, r_j)$ is the change in free energy when both cells, at r_i and r_j are excluded. In other words, an effective attractive interaction exists between the two excluded cells, so that the free energy decreases as the cells approach each other. This effect is due to walks in the unrestricted case which visit both excluded cells, and are therefore not counted in either $c_n^{(1)}(r_1)$ or $c_n^{(1)}(r_2)$. The total force f'_{SAW}, resulting from the simultaneous exclusion of all cells besides the one at the grafting point $r = 0$, must thus be smaller than the force f_{SAW} defined in equation (8). It is easy to find, since the number of SAWs with n steps $d_n^{(1)}$ in this case is given by $d_n^{(1)} = 1 + c_{n-1}^{(1)}$, that for a given value of n the force at the grafting point will be $f'_{n,\mathrm{SAW}} = -\ln(d_n^{(1)}/c_n^{(1)})$. For large n, we obtain $f'_{\mathrm{SAW}} = \ln \mu \approx 0.9701$, smaller than $f_{\mathrm{SAW}} = 1.533$, as expected.

Finally, we should also stress that although the pressure applied by the SAWs and by the Gaussian chains display a similar power-law behavior, other possible walks on the lattice

might lead to different results. Recently, the pressure exerted by directed walks starting at the origin on the limiting line of a semi-infinite square lattice was obtained [24]. In the limit of large directed walks, the asymptotic decay of the pressure with the distance to the grafting point also follows a power law, albeit with an exponent smaller than the one obtained here for SAWs and Gaussian chains.

Acknowledgments

We would like to thank Neal Madras for useful comments. The computations for this work were supported by an award under the Merit Allocation Scheme on the NCI National Facility at the Australian National University. We also made use of the computational facilities of the Victorian Partnership for Advanced Computing. IJ was supported under the Australian Research Council's Discovery Projects funding scheme by the grants DP0770705 and DP1201593. JFS acknowledges financial support by the Brazilian agency CNPq.

References

[1] Ninham B W and Nostro P L 2010 *Molecular Forces and Self Assembly: in Colloid, Nano Sciences and Biology* (Cambridge: Cambridge University Press)
[2] Smith S B, Cui Y J and Bustamante C 1996 *Science* **271** 795
[3] Chaikin P M and Lubansky T C 2000 *Principles of Condensed Matter* (Cambridge: Cambridge University Press)
[4] Safran S 2003 *Statistical Thermodynamics of Surfaces, Interfaces and Membranes* (Boulder, CO: Westview Press)
[5] Tolman R C 1979 *The Principles of Statistical Mechanics* (New York: Dover)
[6] Bickel T, Marques C and Jeppesen C 2000 *Phys. Rev.* E **62** 1124
[7] Bickel T, Jeppesen C and Marques C M 2001 *Eur. Phys. J.* E **4** 33
[8] Breidenich M *et al* 2000 *Eur. Phys. Lett.* **49** 431
[9] Barber M N, Guttmann A J, Middlemiss K M, Torrie G M and Whittington S G 1978 *J. Phys. A: Math. Gen.* **11** 1833
[10] Enting I G 1980 *J. Phys. A: Math. Gen.* **13** 3713
[11] Conway A R, Enting I G and Guttmann A J 1993 *J. Phys. A: Math. Gen.* **26** 1519
[12] Jensen I 2004 *J. Phys. A: Math. Gen.* **37** 5503
[13] De'Bell K and Lookman T 1993 *Rev. Mod. Phys.* **65** 87
[14] Whittington S G 1975 *J. Chem. Phys.* **63** 779
[15] Duplantier B and Saleur H 1986 *Phys. Rev. Lett.* **57** 3179
[16] Duplantier B 1989 *J. Stat. Phys.* **54** 581
[17] Guttmann A J and Whittington S G 1978 *J. Phys. A: Math. Gen.* **11** 721
[18] Guttmann A J 1989 *Phase Transitions and Critical Phenomena* vol 13 (New York: Academic)
[19] Guttmann A J (ed) 2009 *Polygons, Polyominoes and Polycubes* (*Lecture Notes in Physics* vol 775) (Berlin: Springer)
[20] Caracciolo S, Guttmann A J, Jensen I, Pelissetto A, Rogers A N and Sokal A D 2005 *J. Stat. Phys.* **120** 1037–100
[21] Clisby N and Jensen I 2012 *J. Phys. A: Math. Theor.* **45** 055208
[22] Owczarek A L, Prellberg T, Bennett-Wood D and Guttmann A J 1994 *J. Phys. A: Math. Gen.* **27** L919
[23] Rudnick J and Gaspari G 2004 *Elements of the Random Walk* (Cambridge: Cambridge University Press)
[24] van Rensburg E J J and Prellberg T 2012 arXiv:1210.2761